# Physics and Modeling of W7-AS Island Divertor

Y.Feng[1], F.Sardei[1], J.Kisslinger[2], P.Grigull[1], K.McCormick[1], D.Reiter[3]

[1] Max-Planck-Institut für Plasmaphysik, Teilinstitut Greifswald, Euratom Association, 17491 Greifswald, Germany
[2] Max-Planck-Institut für Plasmaphysik, Euratom Association, 85748 Garching, Germany
[3] Institut für Plasmaphysik, Forschungszentrum Jülich Gmbh, Euratom Association, Trilateral Euregio Cluster, 52425 Jülich, Germany

e-mail: feng@ipp.mpg.de

## 1. Introduction

Dedicated high-density experiments in W7-AS operated in the new HDH regime have shown that stable detachment can be achieved in open island divertors if the relevant impurities do not accumulate in the plasma core [1-3]. However, the approach to detachment has shown different signatures from those known from tokamak poloidal field divertors, the most important ones of which being the absence of a high recycling regime, the enhanced parallel drop of the plasma pressure and the need of a very high separatrix density for achieving detachment [4]. These peculiarities of the W7-AS island divertor essentially reflect the prominent role of the cross-field plasma transport in island divertors due to a very small field-line pitch angle. A typically small target-to-core distance further strengthens this role. At the detachment transition, the code predicts a sharp rise of the divertor radiation level and a jump of the radiation zone towards the separatrix, confirmed by the experiment [5]. A stable detachment could be experimentally found only if the target-to-core distance or the field-line pitch were sufficiently large, i.e. the parallel transport not too small compared to the cross-field transport [6]. Both quantities were controlled by external fine-tuning of the island size and radial position. At detachment, the code analysis indicates a stabilisation of the radiation zone at the inboard side of the torus. This inboard-outboard asymmetry of the carbon radiation, which is due to the radial compression of the island surfaces at the low-field side, is responsible for the observed inhomogeneous unloading of the target plates at the detachment transition. In fact, a resulting larger parallel power flow at the low-field side maps onto the target plates preventing detachment at the corresponding strike points. The presented investigations are the result of a close interaction between experiment and modelling in W7-AS. The discussion will include the sensitivity of the observed partial detachment to the island geometry, the dynamic behaviour of carbon radiation, the efficiency of neutral screening in the open island divertor and its impact on detachment stability. The paper addresses the present understanding of the W7-AS island divertor physics as it emerges from global considerations, experimental studies and detailed numerical analysis with the 3D EMC3-EIRENE code [7,8] predicting or reproducing experimental results.

## 2. Island divertor vs tokamak divertor

Although the plasma boundaries of island divertors and tokamak poloidal-field divertors are governed by the same physics, leading geometrical parameters are different, which is reflected in different weights of the transport and recycling processes. For example, the divertor-relevant field-line pitch in the islands is about two orders of magnitude smaller than that of a tokamak divertor. The small pitch is mainly due to the low shear in W7-AS and W7-X. The small pitch explains why $L_c$ for island divertors ($\approx$ 100 m for W7-AS and W7-X) is

generally larger than that for even large tokamaks. The distance between the main plasma and the target plates is also much smaller than in tokamaks, leading to a less efficient screening of the recycling neutrals from the bulk plasma. Both a smaller field-line pitch and a smaller plasma-to-target distance increase the importance of cross-field transport. A further difference is the inherent three-dimensionality of island divertors (see figure 1). It arises from the discontinuity of the target and baffle plates, which defines periodically localized recycling zones along the islands, and from the toroidal variation of the radial island width, which causes inhomogeneous radial transport fluxes. Both effects lead, for low temperatures, to a periodic modulation of the plasma parameters along the islands, which cannot be smoothed out by parallel heat conduction [9].

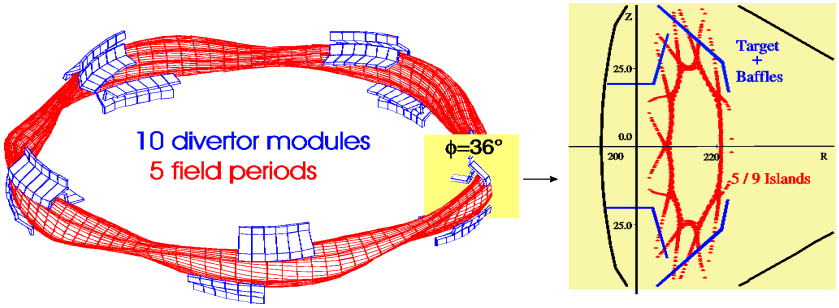


*Fig.1: Island divertor geometry in W7-AS. Ten up/down symmetric divertor modules are installed around the elliptical planes. The standard divertor configuration is the 5/9 configuration, with 9 islands appearing at the edge.*

### 3. Island transport

Numerical studies using EMC3/EIRENE code showed that the transport behaviour of the island divertor differs from that of a tokamak [10]. Compared to tokamaks, the downstream density $n_{ed}$ in W7-AS typically shows a roughly linear scaling with the upstream density $n_{eu}$ indicating no high recycling and never exceeding $n_{eu}$. The downstream temperature $T_{ed}$ decreases with $n_{eu}$ faster than $T_{ed} \propto n_{eu}^{-2/3}$ (linear regime) but slower than $T_{ed} \propto n_{eu}^{-2}$ (high recycling tokamak regime). The upstream temperature $T_{eu}$ drops significantly with $n_{eu}$ even in the case of $T_{ed} << T_{eu}$. The ratio of the downstream and upstream total pressures $2n_{ed}T_{ed}/n_{eu}T_{eu}$ is clearly below unity even at low densities, high temperatures, indicating a significant momentum loss of the plasma ions flowing in the main channel. A dedicated numerical transport study including intrinsic carbon impurities shows that higher upstream densities are needed to achieve detachment as compared to tokamaks, because of the additional momentum losses associated with the island divertor geometry, which have to be balanced by higher upstream pressures [5]. Concerning the physics of detachment, major predictions of the code calculations were a jump of the radiation level and a jump of the radial position of the radiation zone at detachment transition [4]. The first effect is due to a thermal instability associated with the two-branch characteristic of the carbon cooling rate function. By increasing the impurity concentration $C$ or the plasma density $n$ for attached conditions, the temperature at the targets gradually drops approaching a bifurcation point where it jumps from the high-temperature branch to the low-temperature branch of the cooling rate function, indicating detachment transition. The second effect starts at this point and depends on the radial heat transport. As soon as the radiation capability of the impurity at the target $const\sqrt{(2C\chi n^3)_{target}}$ [4] exceeds the power entering the SOL, the radiation zone becomes unstable and detaches form the target. It will stop only if it finds a radial position where the local radiation capability equals the input power. No such stable position of the radiation zone has been found inside the islands so far from both the code calculations and the bolometric

measurements. This process is governed essentially by the radial local power balance between cross-field transport and impurity radiation.

## 4. Deposition patterns

After the implementation of the RFLM-method in the EMC3 code, a realistic interpretation of local experimental data has become possible. In particular, unexpected patterns of the target particle deposition and an asymmetric power unloading of the target at detachment transition could be explained. B-field reversal experiments show a clear dependence of the particle deposition pattern on the B-field direction, indicating the drift effects. E×B drift effects have been modelled with the EMC3/EIRENE code using a simple model neglecting the potential variation on island surfaces to explain the measured poloidal density asymmetries in the islands [11]. The model has been improved by integrating the parallel momentum equation for electron to determine the 3D potential distribution [12]. Cross-field electric currents are still neglected. This implies constant parallel currents which are derived from the potential difference between the two ends of the field lines on the targets. In this model, the E-field is determined from equipotential surfaces and the corresponding E×B drift terms are included in the continuity and momentum equations. These drifts destroy the stellarator symmetry, wherefore the toroidal computational domain had to be extended from one half to one full period. This model reproduces and explains the unexpected particle deposition patterns, namely a strong particle flux in shadowed plate regions.

Impurity radiation reduces the energy flux onto the targets. However, the unloading of the plates is not homogeneous, especially at detachment transition. Typically the plasma does not detach at the plate region which is topologically connected to the low field side of the torus. This behaviour was produced by the simulations and can be explained as follows. The radial field line compression on the outboard side implies a higher radial heat flux than on the inboard side, which leads to a poloidally asymmetric temperature distribution. At detachment, carbon radiation is located on the inboard side due to the lower radial heat flux, which in turn lowers the inboard side temperature. The asymmetry in temperature distribution is the reason for the observed partial detachment.

## 5. Geometry-dependent detachment stability

### 5.1 Experimental observations

Stable partial detachment with more than 80% of the SOL power being radiated at the edge has been achieved in the W7-AS island divertor without significant loss of the global energy confinement. The new HDH-regime [1, 2] found in W7-AS provides a high separatrix density, which is necessary for plasma detachment in the island divertor. Furthermore, the strong decrease of the impurity confinement time in the core of HDH-plasmas [3] prevents the radiation layer from shifting inwards and thereby avoids a radiative collapse. However, divertor experiments have shown that a stable detachment cannot be established for a rather small target-core distance

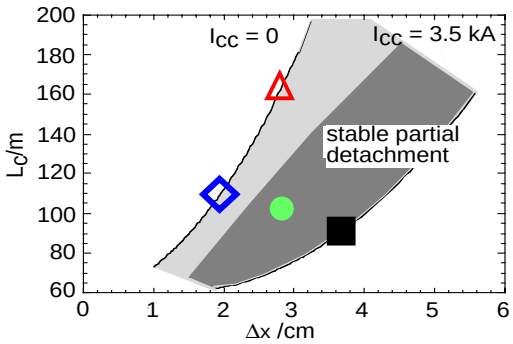


*Fig. 2: Stable partial detachment is restricted to large Δx and small $L_c$ ranges (shadowed region). Four configurations are selected for numeric studies.*

$\Delta x$ or when the connection length $L_c$ becomes too large [6], in spite of the presence of the HDH-regime. Figure 2 shows the location of the stable detachment region in the $\Delta x$-$L_c$ diagram experimentally obtained by proper combination and fine adjustment of the rotational transform ι and control coil current $I_{cc}$.

### 5.2 Simulation results

In the numeric studies the two geometric parameters $L_c$ and $\Delta x$ are varied separately through appropriate choice of four configurations as shown in figure 2. Cross-field transport coefficients are kept fixed through all the computations. Carbon released from the divertor plates through sputtering processes is considered to be the only impurity species, with the yield being linearly coupled with the recycling flux. With a fixed SOL power $P_{sol}$ detachment is achieved in the simulations by increasing the separatrix density $n_{es}$. Then, $n_{es}$ is further increased in small steps until the radiation zone shifts into the core. Figure 3 shows the dependence of carbon radiation on $n_{es}$ for the four selected configurations. With decreasing $\Delta x$ or enlarging $L_c$, the detachment transition shifts to higher densities and the detachment range becomes smaller. Note that both a smaller $\Delta x$ and a larger $L_c$ will increase the weight of cross-field transport.

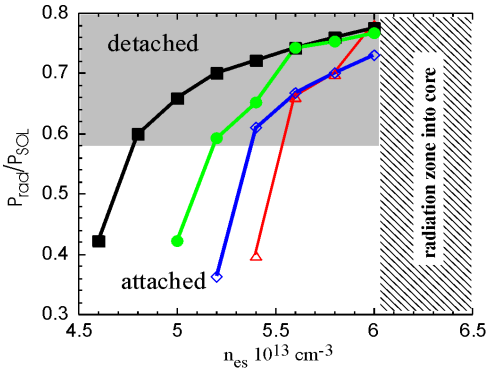


*Fig. 3: Carbon radiation normalized to $P_{sol}$ as a function of $n_{es}$ and configuration.*

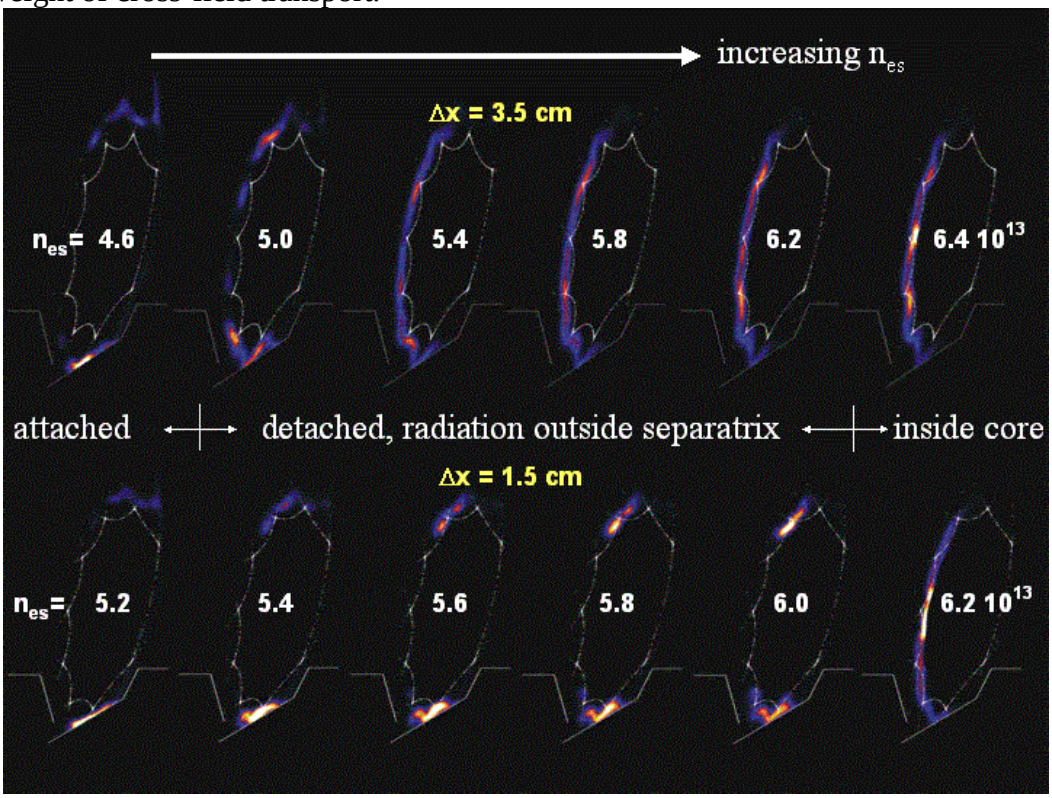


*Fig.4: Evolution of carbon radiation zone through detachment for two different Δx cases.*
*Top: larger Δx, radiation zone moves gradually to X-points on the inboard side with increasing $n_{es}$.*
*Bottom: smaller Δx, radiation zone stays poloidally in divertor region while it moves inwards.*

When detachment occurs the radiation layer detaches from the divertor plates and shifts towards the X-points located just in front of the targets, independent of the configurations selected. Around this X-point the magnetic field lines have the largest radial expansion, which minimizes the cross-field heat transport and thereby favors a radiation condensation. With increasing plasma density, however, the radiation distribution in the island SOL for different configurations develops in two different ways, as shown in figure 4. For the two stable configurations (larger islands and smaller $L_c$, see figure 2), the radiation zone gradually shifts poloidally away from the divertor region to the X-points located on the inboard side of the torus. When $n_{es}$ increases further, the radiation zone extends poloidally to form a radiation belt on the high-field side. At the same time, the radiation belt shifts inward and finally moves into the confinement region. In contrast, the small $\Delta x$ or the large $L_c$ for the two unstable configurations leads to an intensive and strongly localized radiation in the divertor region. Increasing the plasma density causes a much faster inward shift of the radiation zone to touch the closed region than for the inboard side radiation case. Once the radiation zone moves into the core, however, the radiation zone shifts to the inboard side to form a radiation pattern which is almost identical to the first case (see figure 4). The two typical radiation patterns, i.e. inboard side radiation and divertor radiation, for the four selected configurations are compared in figure 5.

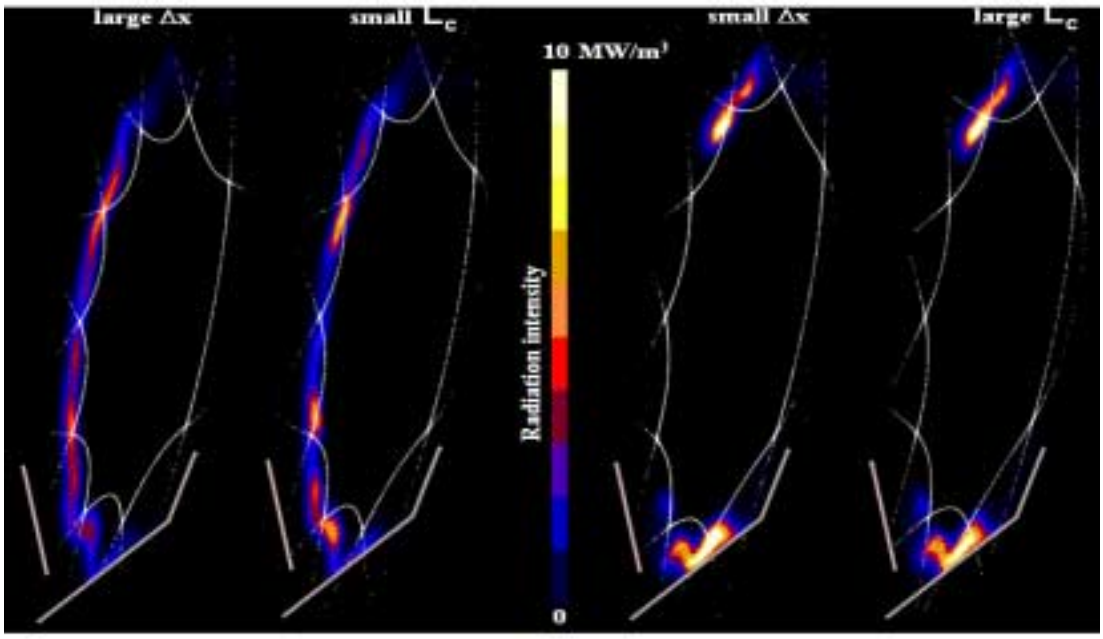


*Fig. 5: Two typical radiation patterns are identified by the code.*
*Left: Inboard side radiation for large $\Delta x$ and small $L_c$*
*Right: Divertor radiation for small $\Delta x$ or large $L_c$*

Experimental data for stable detachments are consistent with the inboard side radiation picture. After transition to a stable detachment, both the He-beam spectrometer viewing a upper divertor region [13] and the bolometer viewing a lower one [14] show a reduction of CIII emission and carbon radiation in the divertor region, although the global carbon radiation jumps to a higher level. Furthermore, at detachment, the divertor plate thermography shows a local hot spot remaining on the divertor plate segments which are magnetically connected to the outside of the torus, being an evidence for the inboard side radiation.

The evolution of the radiation zone in the island divertor is similar to that of MARFEs observed in tokamaks, especially for the divertor radiation case. Nevertheless, whereas an X-

point MARFEs in a tokamak may be stable and can be maintained over a certain density range, a stable detachment related to the divertor radiation picture in the W7-AS island divertor has not yet been established. The reason for this will be discussed in the following section.

### 5.3 Detachment instability driven by neutrals

Divertor radiation lowers the temperature in the recycling zone. As a consequence, the islands become too cold to stop the recycling neutrals. The strong influence of the radiation location on neutral screening efficiency can be clearly seen in figure 6. For the divertor radiation case the neutral penetration flux into the core, $\Gamma_{rc}$ which is normalized to $\Gamma_{NBI}$ of a power of 2 MW, becomes much more sensitive to $n_{es}$ and $P_{sol}$ than for the inboard side radiation case. This means that a small change of $n_{es}$ or $P_{sol}$ can lead to a drastic change of $\Gamma_{rc}$ and thereby introduces a strong perturbation to the particle balance in the core. In fact, such a perturbation comes from the edge as the plasma changes its state from attach- to detachment. Once the transition occurs, $\Gamma_{rc}$ suddenly increases. Because of the density screening effect of the HDH plasma (high density and flat profile), the penetrating neutrals are deposited in the edge region just inside the separatrix, leading to a local rise of density before the particles spread out in the core after a relatively longer time scale characterizing the core transport. This process can be described by the perturbation equation:

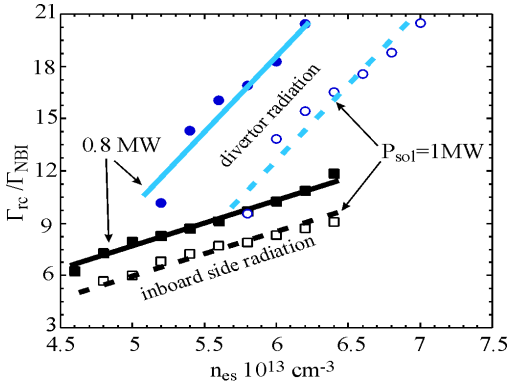


*Fig. 6: Neutral gas penetration flux into the core as a function of $n_{es}$, $P_{sol}$ and configuration calculated by the 3D code.*

$$\frac{\partial \Delta n_e}{\partial t} = \frac{1}{\lambda_0 A_s}\Delta\Gamma_{rc} - D\frac{\Delta n_e}{\lambda_0^2} \qquad (1)$$

where $\Delta\Gamma_{rc}$ is the change of the neutral penetration flux from attach- to detachment, $\Delta n_e$ the corresponding change of the local core density within the neutral penetration depth $\lambda_0$, $A_s$ the last closed flux surface and D the diffusion coefficient for the core. Ignoring the slower core transport and noting that $\Gamma_{rc}$ is a function of $n_{es}$ and $P_{sol}$, we have

$$\frac{\partial \Delta n_e}{\partial t} = \frac{1}{\lambda_0 A_s}\left(\frac{\partial \Gamma_{rc}}{\partial n_{es}}\Delta n_{es} + \frac{\partial \Gamma_{rc}}{\partial P_{sol}}\Delta P_{sol}\right) \qquad (2)$$

where $\partial\Gamma_{rc}/\partial n_{es}$ and $\partial\Gamma_{rc}/\partial P_{sol}$ can be derived from figure 6. Note that $\partial\Gamma_{rc}/\partial P_{sol} < 0$. As $P_{sol}$ decreases with increasing $\Delta n_e$, due not only to the energy loss directly associated with neutrals but also to the increased core radiation resulting from the rise in density, the second term becomes positive and hence destabilizing. The growth rate of this instability is proportional to $|\partial\Gamma_{rc}/\partial P_{sol}|$ which is much larger for the divertor radiation than for the inboard side radiation. Note also the smaller detachment range for those configurations (see figure 3). Decreasing $n_{es}$ has a stabilizing effect on the growth of $\Gamma_{rc}$ (see figure 6) and thereby the instability. The facts that stable detachment can only be established for sufficiently large islands and large field line pitch and the observation of the simultaneous and corresponding drop of $P_{sol}$ and $n_{es}$ through the stable detachment confirm this theory [1].

## 6. Conclusions

Applications of the EMC3/EIRENE code on the W7-AS island divertor have provided several interesting results such as the predictions of the prominent role of the cross-field transport associated with the small islands and field line pitch, additional momentum loss resulting from cross-field diffusion, absence of the high-recycling regime, high separatrix densities needed for achieving detachment and the jump of the radiation level and position at detachment transition. These basic effects have been verified by W7-AS divertor experiments. Implementation of the RFLM-technique in the EMC3/EIRENE code allows a direct link of 3D simulation results with local diagnostics. Interchange between the code and diagnostics is necessary for improvement of code models and for understanding divertor physics. For example, the discrepancy in particle deposition pattern between the code and a $H_\alpha$ camera motivated the implementation of the $E\times B$-drift into the code to explain the particle flows into the shadowed region on the targets. On the other hand, the consistence between the simulated energy deposition pattern and the thermography measurements for partially detached plasmas relates the explanation of the partial detachment physics to asymmetric poloidal temperature and carbon radiation distributions resulting from the code.

Recent studies were aimed at understanding the mechanisms for the geometry-related detachment stability. Island divertor experiments show that a stable detachment requires sufficiently large islands and field line pitch. Numeric studies show that, under detachment condition, the radiation distribution in the island SOL is sensitive to the island geometry. Two typical radiation patterns are identified from the simulations, namely the inboard side radiation for large islands with large field line pitch and the divertor radiation for small islands with small field line pitch. Divertor radiation lowers the temperature in the recycling zone such that the islands become too cold to stop the recycling neutrals. A linear stability analysis based on 3D simulation results shows that a sudden increase of neutral penetration flux into core at detachment transition drives an instability, with a growth rate being directly related to the neutral screening efficiency. Decreasing the edge density has a stabilizing effect. These results are consistent with the experimental observations.

## References


[1] P. Grigull et al., 2001 *Plasma Phys. Contr. Fusion* **43** A175
[2] K. McCormick et al., *PRL* **89** 015001
[3] R. Burhenn et al., 2002 *29th EPS Conf.* (Montreux)
[4] Y. Feng et al., 2001 *Plasma Phys. Contr. Fusion* **44** 611
[5] Y. Feng, F. Sardei, J. Kisslinger, D. Reiter, Y. Igitkhanov, 2001 *28th EPS Conf.* (Madeira)
[6] P. Grigull et al., this conference
[7] Y. Feng, F. Sardei, J. Kisslinger, 1999 *J. Nucl. Mater.* **266-269** 812
[8] D. Reiter, 1984 *Technical Report* Jül-1947, KFA Jülich, Germany
[9] F. Sardei et al., 1997 *J. Nucl. Mater.* **241-243** 135
[10] Y. Feng, J. Kisslinger, F. Sardei, 1999 *26th EPS Conf. (Maastricht)*
[11] Y. Feng, G. Herre, P. Grigull, F. Sardei, 1998 *Plasma Phys. Contr. Fusion* **40** 371
[12] Y. Feng et al., 2003 *J. Nucl. Mater.* **313-316** 857
[13] N.Ramasubramanian et al., 2003 *30th EPS Conf.* (St. Petersburg)
[14] L. Giannone et al., 2003 submitted to *PPCF*